Netrin-1 inhibits sprouting angiogenesis in developing avian embryos.

Karine Bouvrée, Bruno Larrivée, Xiang Lv, Li Yuang, Benjamin Delafarge, Catarina Freitas, Thomas Mathivet, Christiane Bréant, Marc Tessier-Lavigne, Andreas Bikfalvi, et al.

Netrin-1 inhibits sprouting angiogenesis in developing avian embryos

Karine Bouvrée[1,2], Bruno Larrivée[1,2,], Xiang Lv[3], Li Yuan[4], Benjamin DeLafarge[1,2], Catarina Freitas[1,2,], Thomas Mathivet[1,2,], Christiane Bréant[1,2], Marc Tessier-Lavigne[5], Andreas Bikfalvi[6,7], Anne Eichmann[1,2,] and Luc Pardanaud [1,2,$]

[1]*Inserm, U833, F-75005 Paris, France*

[2]*Collège de France, 11, Place Marcelin Berthelot, F-75005 Paris, France*

[5]*Genentech Inc., 1 DNA Way, South San Francisco, CA 94080*

[6]*Inserm, U920, Avenue des Facultés, 33405 Talence*

[7]*Université Bordeaux I, Avenue des Facultés, 33 405 Talence*

[$]*Corresponding author, email:* luc.pardanaud@college-de-france.fr*, tel: 33-1-44271646, fax: 33-1-44271691*

[3]*present address: Beijing Union Medical College & Chinese Academy of Medical Sciences, Beijing, China*

[4]*present address: School of Life Sciences, Xiamen University, China*

Running title: Netrin-1 inhibits angiogenesis

Key words: vessel guidance, UNC5B, angiogenesis, sprouting, CEC/EPC

Abstract

Netrin-1 is a bifunctional axonal guidance cue, capable of attracting or repelling developing axons via activation of receptors of the deleted in colorectal cancer (DCC) and uncoordinated 5 (UNC5) families, respectively. In addition to its role in axon guidance, Netrin-1 has been implicated in angiogenesis, where it may also act as a bifunctional cue. Attractive effects of Netrin-1 on endothelial cells appear to be mediated by an as yet unknown receptor, while repulsion of developing blood vessels in mouse embryos is mediated by the UNC5B receptor. To explore evolutionary conservation of vascular UNC5B expression and function, we have cloned the chick *unc5b* homologue. Chick and quail embryos showed *unc5b* expression in arterial EC and sprouting angiogenic capillaries. To test if Netrin-1 displayed pro- or anti-angiogenic activities in the avian embryo, we grafted cell lines expressing recombinant chick or human Netrin-1 at different stages of development. Netrin-1 expressing cells inhibited angiogenic sprouting of *unc5b* expressing blood vessels, but had no pro-angiogenic activity at any stage of development examined. Netrin-1 also had no effect on the recruitment of circulating endothelial precursor cells. Taken together, these data indicate that vascular *unc5b* expression and function is conserved between chick and mice.

Introduction

The vertebrate vascular system is a highly organized, branching network of arteries, capillaries and veins that penetrates virtually all body tissues. The vasculature forms during early embryonic development when endothelial cell (EC) precursors called angioblasts differentiate and coalesce into solid cords of the primary vascular plexus, a process known as vasculogenesis (Conway et al., 2001). New vessels subsequently grow from this primitive network, by either sprouting from parent vessels (sprouting angiogenesis) or by intravascular subdivision (non-sprouting angiogenesis). Vascular development has been extensively studied in avian embryos, due to the relatively large size of the embryo and the easy access at different developmental stages, which allows experimental manipulations. For example, the chorioallantoic membrane (CAM), a highly vascularized extraembryonic tissue, has been extensively used to study effects of angiogenic growth factors or to follow tumor vascularization (Hagedorn et al., 2005). In addition, generation of quail-chick chimeras allows tracing of endothelial cells (EC) derived from quail grafts in the chick host using the monoclonal antibody QH1, which recognizes quail EC and hematopoietic cells (HC) only (Pardanaud et al., 1987, 1996).

The vascular system shares several anatomical and functional parallels with the nervous system. Both systems utilise a complex branching network of nerve cells or blood vessels to penetrate all regions of the body. Pathfinding of axons in the nervous system is achieved by the growth cone, a sensory structure present at the leading tip of extending axons, which integrates directional information provided by attractive and repulsive guidance cues in the surrounding environment (Dickson, 2002). Recent work has demonstrated that sprouting capillaries are also guided by specialized EC called tip cells, which perform an analogous function to growth cones (Gerhardt et al., 2003; Isogai et al., 2001). Tip cells, like growth cones, continually extend and retract numerous filopodia to explore their environment, and function to define the direction in which the new vascular sprout grows. The behavioral similarities between the axonal growth cone and endothelial tip cell are complemented by the fact that both systems use a common repertoire of molecular ‘sensors’, i.e., ligand/receptor signaling systems, which couple the guidance cues detected in the external environment with the cytoskeletal changes necessary to alter cell direction. Among the axon guidance cues that have been identified as regulators of vascular development are Netrins.

Netrins are laminin-related secreted molecules, which bind to members of the UNC5 and DCC receptor families. Netrins are involved in both attraction and repulsion of neurons,

depending on the receptor types that are expressed (Chisholm and Tessier-Lavigne, 1999). For example, Netrin-1 attracts dorsal commissural interneurons through DCC receptors, but repels certain classes of motor neurons through UNC5 receptors (Chisholm and Tessier-Lavigne, 1999). UNC5 receptors form homodimers to mediate short-range repulsion by Netrin, but need to heterodimerise with DCC to mediate longer-range repulsion (i.e., at low concentrations) (Kennedy, 2000).

In addition to their role in axon guidance, Netrins and their receptors have been implicated in other developmental processes including angiogenesis (Cirulli and Yebra, 2007). Netrins may also act as bifunctional cues during angiogenesis. Wilson et al. (Wilson et al., 2006) have provided evidence for pro-mitogenic and pro-migratory effects with Netrin-1 and -4 *in vitro* and pro-angiogenic effects for both Netrins in post-ischemic revascularization processes via unidentified receptor(s). In contrast, we have previously observed repulsive actions of Netrin-1 via UNC5B in developmental angiogenesis (Lu et al., 2004). UNC5B, one of four mammalian UNC5 receptors, is expressed in arteries, a subset of capillaries, and on endothelial tip cells and genetic deletion of this receptor in mice results in excessive vessel branching and increased extensions of tip cell filopodia. *In vivo* treatment of growing vessels with Netrin-1 induces filopodial retraction in wildtype mice but not in UNC5B-deficient mice, suggesting that Netrin-1 inhibits vessel branching. To further explore the evolutionary conservation of vascular UNC5B expression and function, we report herein cloning of the chick *unc5b* homologue and its expression in developing blood vessels. Stimulation of *unc5b* expressing blood vessels in the CAM by Netrin-1 inhibited vessel sprouting, while Netrin-1 had little activity on the migration of angioblasts, of which only a minority expressed *unc5b*.

Materials & Methods

Cloning of chick unc5b

A fragment of chick *unc5b* was cloned using total RNA extracted from 9-day old (E9) chick embryos and 0.5 µg were reverse transcribed using 100 pmol OligodT23VN and 200 U of SuperscriptII (Clontech) in a 20 µl reaction. PCR was carried out on 2 µl RT using 12 pmol of the following primers: 5'TGAGTACAGCCTCAAGGTCTACTG and 5' CTAGGTTGTACTCGTCTCTTCAAC in a 25 µl reaction 95°C/2'- (95°C/20''- 68°C/4'') x 35-72°C/7'-4°C using an iCycler (BioRad). The resulting 1035bp PCR product corresponding to nt 2220-3253 of the chick *unc5b* sequence (AF380352) was ligated to pCRII-Topo.

In situ hybridization and Immunohistochemistry

In situ hybridization (ISH) on whole-mounts and sections was done as described previously (Moyon et al., 2001) using *unc5b* and a fragment of quail *vegfr2* (Eichmann et al., 1996). Double staining with QH1 (Pardanaud et al., 1987) was done as described (Moyon et al., 2001). Whole-mount QH1 staining and QH1/glychemalun staining was performed as described (Pardanaud et al., 1987, Pardanaud and Eichmann, 2006).

Protein application on CAM

Recombinant chicken Netrin-1 and human $VEGF_{165}$ (R&D) were diluted in PBS 0,1% BSA. Fertilized chicken eggs (*Gallus gallus,* JA57) were incubated at 37°C and 80% humidified atmosphere. At E2 a window was made in the shell and sealed with scotch tape. FITC Dextran (MW 2.10^6, SIGMA) was intravenously injected to visualize the CAM vessels, then to observe the vascular response, Indian ink diluted in PBS (1/1) was injected beneath the CAM to get an artificial dark field. Ten µl containing 1 µg of protein (cNetrin-1 or hVEGF) were directly applied at E10 on the CAM surface, inside a silicon ring (inside diameter = 5 mm, Weber Métaux Plastiques).

Preparation of VEGF-coated beads

Heparin acrylic beads (Sigma) were washed in PBS with calcium/magnesium and incubated one hour at room temperature in recombinant human VEGF (0.5 µg/µl) before grafting.

Cell lines

Human embryonic kidney (HEK) 293 cells stably transfected with chick *netrin-1* (cNetrin-1) or with control vector were described previously (Shirasaki et al., 1996). HEK cells expressing VEGF were generated by transfection of HEK cells with a vector encoding murine *vegf* (pBlast49-mVEGF, Invivogen) and subsequent selection using blasticidin (1 mg/ml, Invivogen, Di Marco et al., submitted). MiaPaCa, Mel2a and PC3 tumor cell lines retrovirally transduced with a construct encoding human *netrin-1* (hNetrin-1) were described (Larrivee et al., 2007). All cells were cultured in Dulbecco's modified eagle medium (DMEM, GIBCO) containing 10% fetal bovine serum (GIBCO) and penicillin-streptomycin (GIBCO).

To determine levels of Netrin-1 secretion, $7.5x10^5$ cells were plated overnight in a 10 cm Petri dish followed by 48 hours culture in serum-free DMEM. Supernatant was harvested and incubated overnight at 4°C in ELISA plates coated with anti-human IgG1 (1.8 µg/ml, Jackson laboratories), saturated with PBS 1% BSA, then coated with 200 ng/ml UNC5B/Fc chimera (R&D). Plates were washed in Tris-buffered saline 0,05% Tween 20 (Sigma) and incubated for 2 hours with anti-His-HRP (1/5000, Roche). After further washes, plates were incubated with 0.1 mg/ml 3, 5, 3', 5'-tetramethylbenzidine for 15 minutes and the reaction was stopped by addition of 1M H_2SO_4. Absorbance at 450 nm was read on a microplate reader (Dynatech MR5000) with wavelength correction set at 540 nm. For mouse and endogenous human VEGF ELISA assay we used the Duoset Kit (R&D). For Western blot analysis culture supernatants were concentrated using an Amicon Ultra Centrifugal Device (Millipore). Twenty µl of 500 µl concentrated supernatant was separated on SDS-PAGE (Invitrogen) and transferred to PVDF membranes (Millipore). Membranes were blocked with 5% milk in PBS/0,1% Tween 20 (Sigma), incubated with primary antibodies (1/1000, R&D) and developed by enhanced chemoluminescence (Pierce). For grafts of cell aggregates into early embryos, cells were plated on a semisolid medium in a 35 mm Petri dish and left to form aggregates for 36 hours.

Human cell grafts on CAM

E9 chick or quail eggs (*Coturnix coturnix japonica*) were used (Hagedorn et al., 2005). The CAM surface was gently lacerated and a silicon ring (inside diameter=10 mm) was placed on

the CAM. Twenty µl (3.10^6 cells) of suspension (Mel2A and HEK) in culture medium were deposited inside the ring. After 3 or 6 days the CAM was sectioned around the ring, carefully cleaned in PBS and fixed few hours in absolute alcohol/1% acetic acid at -20°C or overnight in PAF4%, embedded in paraffin, sectioned and stained.

Human tumor cell grafts in parabioses

Parabiotic embryos were generated as previously described (Wong and Ordahl, 1996) by pouring an E2 quail embryo in an E2 chick egg through a window in the shell. After 7 days of incubation, a silicone ring (inside diameter= 10 mm) was placed on the E9 parabiotic chick CAM after laceration. Suspensions of Mel2A, MiaPaCA or PC3 cell lines (20µl=3.10^6 cells) were deposited inside the ring. The surviving parabioses (118/389=30%) were sacrificed after 3, 6 or 7 days, the latest stage before the quail hatched. The chick CAM was fixed in absolute alcohol/1% acetic acid at -20°C or in 4%PAF, embedded in paraffin, sectioned and stained.

Quail-chick chimeras

Axial structures of E2 chick embryos were ablated as described (Klessinger and Christ, 1996). Indian ink diluted in PBS (1/1) was injected underneath the embryo to facilitate visualization, then the neural tube and notochord were removed over a length of 3 somites with a sharpened microscalpel. The left medial somite along the ablation was also removed. The ablated chick somite was replaced by one quail somite, isolated by enzymatic treatment as previously described (Pardanaud et al., 1996), and the ablated neural tube was replaced by a cell aggregate (neo- or hNetrin-1-infected Mel2A, neo-, mVEGF- or cNetrin-1 transfected HEK). Control ablations with no cellular grafts were also performed. After 2 days of incubation, the embryos were sacrificed, fixed two hours in absolute alcohol/1% acetic acid at -20°C, embedded in paraffin, sectioned and stained.

Grafting experiment at E1.5

An artificial dark field was made beneath E1.5 quail blastodisc (1-5 somite-stage) by Indian-ink injection. After removal of the vitelline membrane, a small incision was performed laterally to the sinus rhomboidalis using a sharpened microscalpel, without touching the endoderm. A cell aggregate was inserted in the cavity and the egg was returned to the incubator for one night. The embryo was then isolated and fixed in absolute alcohol/1% acetic acid at -20°C or in PAF and embedded in paraffin.

Quantification of chick EC and quail QH1$^+$ cells

Observation and counting was done using a Leica microscope. For each harvested graft, serial sections were prepared and nuclei were stained with glychemalun. The size of nodules formed by grafted cells was calculated using a micrometric scale by measuring the surface of the first section where a nodule was visible plus one section per slide multiplied by the thickness of all sections containing nodules (n x 7,5 µm). The number of total chick EC nuclei was counted manually (X25 objective, final magnification X110, 3 sections counted by row) on a total of 5700 sections ($\pm$ 250 000 cells). Quail EC ($\pm$ 32000 cells) and HC ($\pm$ 51000 cells) were counted in the same way after QH1 immunostaining. All cell numbers are expressed as mean±s.e.m. Statistical analyses were carried out using Mann-Whitney U test. $P<0.05$ was considered significant.

Results

Cloning and expression of chick *unc5b*

A 1035 bp fragment of chick *unc5b*, encompassing 700 nt of coding sequence and extending into the 3'UTR was PCR amplified from chick embryo mRNA and cloned. Sequence analysis confirmed that the amplified fragment showed 100% identity with the published chick *unc5b* sequence (AF380352). Chick and mouse *unc5b* coding sequences share 83% amino acid identity.

To examine *unc5b* expression in avian embryos, we performed *in situ* hybridization (ISH) with sense and antisense *unc5b* riboprobes on chick and quail embryos at different developmental stages. Sense probes showed no detectable signal (not shown). Whole-mount ISH of early embryos (1-11 somite stage) showed mesodermal *unc5b* expression in the posterior primitive streak and cardiac crescent, but no specific expression in the neural tube (Fig. 1A-C). 15-25 somite stage embryos showed arterial *unc5b* expression in the dorsal aorta and forming vitelline arteries (Fig. 1D). Consistent with the results obtained by whole-mount ISH, hybridization of antisense riboprobes to sections of E3 chick embryos showed robust *unc5b* labeling of the dorsal aorta and side branches and absence of expression in the neural tube (Fig. 1E). Comparison with *vegfr2* expression showed that both genes labeled arterial endothelium, but *vegfr2* was also expressed in the cardinal vein and in migrating angioblasts (Fig. 1F). Venous cells were negative for *unc5b*, and expression in migrating angioblasts was only detected in a minority of cells (Fig. 1E). Double labeling of sections prepared from E3.5 and E5.5 quail embryos with *unc5b* and QH1, a monoclonal antibody specific for quail EC and hematopoietic cells (HC, Pardanaud et al., 1987) confirmed that *unc5b* was expressed in EC (Fig. 1G, H). Expression levels were highest in branching vessels such as aortic side branches or vessels invading the neural tube and the limb bud (Fig. 1G, H and data not shown). ISH at late embryonic stages showed that mature EC in the E10-E13 CAM exhibited very low *unc5b* expression levels (Fig. 1I). Stimulation of neovessel sprouting by grafting of tumor cells onto the CAM led to up-regulation of *unc5b* in sprouting vessels (Fig. 1J). Taken together, our analysis of *unc5b* expression during avian embryonic development shows that this receptor is prominently expressed on arterial EC and sprouting vessels during the period of active developmental angiogenesis, similar to the expression pattern seen in the mouse (Larrivee et al., 2007; Lu et al., 2004).

Recombinant chick Netrin-1 induces plasma leakage on the CAM

Biological activity of recombinant Netrin-1 on the chick CAM has previously been reported (Park et al., 2004). In that study, application of 1 µg of recombinant chick Netrin-1 or human $VEGF_{165}$ onto the E8 CAM were both reported to potently induce angiogenic vessel sprouting. As expression levels of the repulsive *unc5b* receptor on CAM vessels between E10 and E13 were low, we reasoned that Netrin-1 might induce pro-angiogenic responses in these vessels via other receptors.

We first repeated the experiments reported in Park et al. (2004), using 1 µg of recombinant chick Netrin-1 or human recombinant $VEGF_{165}$. Growth factors were applied onto the CAM surface and vessel response was monitored at different time points post-application under bright light or after intravascular injection with FITC dextran. As shown previously (Wilting et al., 1993), VEGF led to robust capillary vessel sprouting that was already detectable 24 hours post-application (Fig. 2A, B). In contrast, about half of the Netrin-1 treated CAMs (n=13) showed no response (not shown) while the other half formed fibrous nodules surrounded by radial vessel structures growing towards the nodule (Fig. 2C). While these responses resembled those reported previously (Park et al., 2004), radial vessel patterns and nodule formation were never observed after VEGF application. To determine possible causes of nodule formation, we analyzed vessel response immediately after Netrin-1 application by intravascular FITC injection. Strikingly, Netrin-1 induced plasma leak and almost complete disappearance of intravascular fluorescent label within 15-30 minutes (Fig. 2D, E). The effect was strictly localized to the application area and no plasma leak occurred in other regions of the same CAM (Fig 2F). Plasma leakage was only observed at high concentrations of Netrin-1 (1 µg), whereas lower doses (100-500 ng) did not induce leakage or other effects on vessel morphology (not shown). As plasma leak may liberate inflammatory mediators, the observed vascular pattern and fibrous nodules formed in response to Netrin-1 application are likely to be a secondary effect.

HEK cells secreting chick Netrin-1 do not form nodules on the CAM

As acute delivery of Netrin-1 protein at concentrations known to activate UNC5B and other Netrin receptors (50-300 ng/ml, Larrivee et al., 2007; Leonardo et al., 1997) did not provoke any obvious vascular responses on the CAM, we decided to use a cell-based protein delivery system. We grafted matched pairs of stably transfected HEK cells expressing vector only,

vector encoding c*netrin-1* (Shirasaki et al., 1996) or m*vegf*. Western blotting and Elisa measurements of supernatants from the three cell lines showed that Netrin-1 transfected cells secreted 1.1±0.5 µg/ml of cNetrin-1 over a period of 48 hours, while HEK VEGF cells (Di Marco et al., submitted) secreted 13.9± 0.6 ng/ml of mVEGF. Production of endogenous human VEGF was similar between control and Netrin-1 transfected HEK cells (0.2 ng/ml). Proliferation of VEGF or Netrin-1 expressing HEK cells *in vitro* was highly similar (data not shown).

HEK cells were grafted onto E9 quail CAMs ($3x10^6$ cells/egg). Intravascular FITC dextran injection performed after 4 and 24 hours showed no plasma leak after grafting of HEK cells secreting cNetrin-1 (not shown). Grafts were harvested after 3 or 6 days, photographed, fixed and serial sections were prepared. Depending on their vascularization by host blood vessels, the grafted cells formed nodules of varying sizes (Fig. 3A-C). The size of the nodules was calculated and the number of EC inside the nodules was counted after QH1 staining (see Methods).

HEK cells transfected with control vector formed a sheet of cells that remained on the CAM surface at both 3 (n=6) and 6 days (n=5) post-implantation (Fig. 3A). $QH1^+$ quail blood vessel sprouts started invading the sheet of cells at 3 days (Fig. 3F) and EC number increased significantly over the next 3 days (Fig. 3D). Concomitantly with blood vessel invasion, the thickness of the cell sheet and its overall size increased from day 3 to day 6 (Fig. 3E). In contrast to control HEK cells, cNetrin-1 expressing HEK cells only formed tiny nodules on the CAM surface (Fig. 3B, E). Sectioning and QH1 staining showed that most HEK Netrin-1 cells were necrotic after 3 (n=4) and 6 days (n=4) post-implantation and that invasion of vessels into the nodules was greatly decreased compared to control HEK cells (Fig. 3D-G). Some signs of inflammation, i.e., swelling and increase of thickness, together with appearance of $QH1^+$ HC were present in the CAM underneath the cNetrin-1 expressing cells, but vessel sprouting into the nodules was essentially absent (Fig. 3G). In striking contrast to cNetrin-1 expressing HEK cells, mVEGF expressing HEK cells formed large nodules that contained numerous blood vessels visible upon dissection at both day 3 (n=7) and day 6 (n=6) post-implantation (Fig. 3C, D, H). Measurement of nodule size and counting of the number of $QH1^+$ EC within the nodules confirmed that mVEGF expressing cells formed larger nodules with a higher number of blood vessels compared to control HEK cells, while cNetrin-1 expressing HEK cells formed small nodules virtually devoid of blood vessels (Fig. 3D, E).

Tumor cell grafts on parabiotic embryos

To extend these observations to other cell lines, we used three matched pairs of tumor cell lines, Mel2A melanoma cells, MiaPaCa pancreatic tumor cells and PC3 prostate carcinoma cells that were retrovirally transduced with a control virus encoding the neomycin resistance gene or with h*netrin-1* (Larrivee et al., 2007). Our previous analyses had shown that transduced Mel2A cells secreted about 100 ng/ml of hNetrin-1, MiaPaCa cells about 150 ng/ml, while PC3 produced about 20 ng/ml of Netrin-1. Proliferation and clone forming ability of the retrovirally transduced tumor cell lines was highly similar between hNetrin-1 transduced and control-transduced tumor cell lines, indicating that hNetrin-1 expression did not alter the behavior of transduced cells *in vitro* (Larrivee et al., 2007).

The three matched pairs of tumor cells ($3x10^6$ cells/egg) were grafted onto the chick CAM of parabiotic embryos at E9 and invasion of the chick host vessels into the nodules was assessed. In addition to examination of tumor vascularization and growth, the use of parabiotic embryos allows to monitor the participation of circulating endothelial cells/endothelial progenitor cells (CEC/EPC) originating from the parabiotic quail to neovessel formation, and to test possible effects of Netrin-1 on these cells.

For parabioses, an E2 quail embryo with its yolk was transferred into an E2 chick egg. After several days, the two CAMs establish contact and develop vascular connections between the embryos, allowing CEC/EPC to circulate between quail and chick from E8 onwards (Pardanaud and Eichmann, 2006). Tumor cell grafts on the chick CAM were harvested after 3 and 6 (Mel2a, MiaPaCa and PC3) or 7 days (PC3). They were analyzed after fixation in alcohol/1% acetic acid, which results in histologically detectable EC nuclei that can be counted after glychemalun nuclear staining (Fig. 4). CEC/EPC originating from quail were detected using the QH1 monoclonal antibody (Fig. 5).

All three neo-transduced human cell lines formed solid tumors on the CAM as soon as 3 days after grafting (Fig. 4A-C). Each cell line formed morphologically and histologically distinct tumors, with growth characteristics that differed according to the origin of the cell line. Ectomesodermal Mel2A cells (n=21) formed vascularized discs at the surface of the CAM (Fig. 4A, D). In contrast, endomesodermal MiaPaCa cells (n=18) formed large diverticulated tumors. Histological analysis showed that growth of these tumors involved folding up of the CAM and invagination of the endoderm inside the tumor, giving rise to a nodule that distantly resembled an exocrine pancreatic gland (Fig. 4B, E). Endomesodermal PC3 cells (n=23) grew inside the CAM towards the endoderm and gave rise to large, often hemorrhagic tumor

nodules (Fig. 4C, F). Hemorrhage was due to the presence of a large intratumoral vesicle that was filled with erythrocytes, became leaky and finally broke providing superficial hemorrhages (Fig. 4F). Thus, tumor cell lines on the CAM gave rise to nodules with distinct morphology that appeared to reflect, as least to some extent, the embryonic origin of the cell line.

On sections, human tumor cells were easily distinguished from avian cells by their larger nuclei (Fig. 4G-I). All tumors were vascularized by angiogenic sprouting from the chick CAM. Mel2A tumors were vascularized by radially growing, thin vessels that contained HC (Fig. 4 G). MiaPaCa tumor vessels had thin or wide lumens filled with erythrocytes (Fig. 4H). Vessels invading PC3 tumors had wide lumens filled with erythrocytes. At the edge of the intratumoral vesicle, the endothelium often broke, delivering erythrocytes inside (Fig. 4I). Peritumoral lymphatic vessels were readily seen in MiaPaCa (Fig. 4H) and PC3 tumors, but were not visible in Mel2A tumors (not shown).

hNetrin-1 inhibited sprouting angiogenesis but had no effect on CEC/EPC recruitment

hNetrin-1 expression did not alter the gross morphological and histological appearance of tumors formed from the three cell lines (not shown). However, compared to neo tumors, Mel2A/hNetrin-1 and PC3/hNetrin-1 tumors (n=18 each) showed reduced vascularization and growth. Counting of the total number of EC on serial sections showed that Mel2A/hNetrin-1 and PC3/hNetrin-1 tumors contained a lower number of EC compared to Mel2A/neo and PC3/neo tumors (Fig. 4J). Consistent with their reduced vascularization, the volume of Mel2A/hNetrin-1 and PC3/hNetrin-1 tumors remained smaller compared to the corresponding neo tumors (Fig. 4K).

With MiaPaCa/hNetrin-1 tumors (n=19), the total number of chick EC was reduced after 3 days compared to control neo-transduced cells (Fig. 4J). At 6 days, the total EC number was identical in the two tumor types, indicating that the repulsive effect of hNetrin-1 was transient in these tumors. No statistically significant difference was observed for the volume between control and hNetrin-1-producing cells (Fig. 4K).

QH1 staining of tumors grafted on parabiotic embryos allowed us to assess the participation of CEC/EPC to tumor neovascularization, by following the distribution of $QH1^+$ CEC/EPC originating from the quail embryo in the tumors grafted on the chick CAM. $QH1^+$ CEC/EPC reached the chick CAM as previously described (Pardanaud and Eichmann, 2006) together

with $QH1^+$ HC, in particular inflammatory cells that gathered with chick HC beneath the growing tumors (not shown). The majority of $QH1^+$ CEC/EPC invading the tumors were interstitially located (75%, Fig. 5A), the remaining cells integrated endothelia (Fig. 5B). $QH1^+$ HC also colonized the tumors, both inside and outside the vessel lumen (Fig. 5C). Counting of the total number of intratumoral $QH1^+$ CEC/EPC showed no difference between hNetrin-1 expressing and control transduced tumor cells (Fig. 5D), indicating that hNetrin-1 plays no detectable role in the mobilization or homing of $QH1^+$ CEC/EPC to tumor nodules. The participation of $QH1^+$ CEC/EPC to tumor vascularization was low (Fig. 5D, compare with Fig. 4J), their number and density (7-19 $QH1^+$ CEC/EPC/mm^3) attaining levels similar to the ones seen in other embryonic tissues (Pardanaud and Eichmann, 2006). Whatever the tumor cell line or the age of tumors the number of $QH1^+$ CEC/EPC never exceeded 3.3 % of total intratumoral EC, indicating that EPC incorporation *per se* is unlikely to directly contribute to an increase in total vessel density during tumor neovascularization.

Taken together, of four matched pairs of cell lines expressing or not hNetrin-1 (HEK, Mel2A, MiaPaCa and PC3), one cell line, MiaPaCa tumor cells, showed a slight reduction in angiogenesis, while three showed a significant decrease in growth and reduced vascularization. Expression of *unc5b* mRNA was up regulated in vessel sprouts invading control-neo transduced tumors (Fig. 1J, 6A, C), and the number of *unc5b* expressing vessel sprouts was decreased in Netrin-1 producing tumors, consistent with a repulsive effect of Netrin-1 on *unc5b* (Fig. 6B, D). Pro-angiogenic effects of Netrin-1 were not detected in these experiments, but could be readily seen with VEGF.

Effects of Netrin-1 on angioblast migration

To further explore activity of Netrin-1 during avian vascular development, we decided to test effects of Netrin-1 on angioblast migration. In a first series of experiments, we removed the neural tube and notochord from chick embryos and grafted HEK cells expressing cNetrin-1 or mVEGF or Mel2a/neo- or hNetrin-1-transduced tumor cells in place of the ablated tissue. The neural tube and notochord form a barrier that impairs EC located on one side of the embryo from migrating to the contralateral side (Klessinger and Christ, 1996). Removal of the neural tube and notochord allows migration. We thus asked if Netrin-1 or VEGF delivered in place of the neural tube/notochord by the cell aggregates could influence EC migration (Fig. 7). To follow angioblast migration, a chick somite adjacent to the removed neural tube was replaced by a quail somite as a source of EC (Fig. 7A, B). Grafted embryos

were sacrificed after 2 days, and serial sections through the entire trunk region, including the operated region (Fig. 7B, D) and several hundred micrometers rostrally and caudally were prepared (Fig. 7E, F). All sections were stained with QH1/glychemalun to detect all quail EC originating from the grafted somite, which are known to migrate large distances in the embryo (Noden, 1988). When no cells were grafted axially, about 20% of $QH1^+$ EC originating from the quail somite migrated from the left to the right side, indicating that the ablation had removed the endogenous barrier (Fig. 7C). Grafts of control HEK cells led to an equivalent result with 20±9% of $QH1^+$ EC found on the contralateral side (Fig.7 C, E). Grafts of mVEGF-producing HEK cells resulted in a slightly increased number of cells (26±7%) on the contralateral side (Fig. 7C). Grafts of cNetrin-1-producing HEK resulted in a reduction of the percentage (7±5%) of $QH1^+$ EC migrating in the contralateral side (Fig. 7C, F). However, the same experiment performed with Mel2a control or hNetrin-1 expressing cells showed no difference between control- and Netrin-1-transduced cells (Fig. 7C).

In a second series of experiments, quail embryos between the 1- and the 5-somite stage were grafted with the matched HEK or Mel2A control- or Netrin-1-expressing cell aggregates at the level of the *sinus rhomboidalis,* where angioblasts migrate and coalesce to form the primary vascular plexus at these stages. Embryos were left to develop for 18 hours and processed for QH1 immunohistochemistry to quantify angioblast migration in response to Netrin-1. As a positive control, whole-mount QH1 staining after grafts of VEGF-coated beads showed angioblast migration and coalescence around the bead (Fig. 8A), as expected from previous studies (Drake et al., 2000; Drake and Little, 1995). Control Mel2A tumor cells grafts were also surrounded by EC sprouts that approached and sometimes entered the cell mass, although these sprouts were less abundant compared to VEGF (Fig. 8B). Grafts of Mel2A Netrin-1 producing cells appeared to repel EC sprouts (Fig. 8C). However, quantification of EC surrounding cell grafts on sections (Fig. 8D, E) showed no statistically significant difference between Mel2A/neo and Mel2A/Netrin-1 expressing cells (Fig. 8E). The number of EC surrounding HEK control or hNetrin-1 expressing cells was also similar (Fig. 8E), indicating that Netrin-1 had neither repulsive nor attractive activity on early embryonic angioblasts and no effects on EC division.

Discussion

We here describe cloning of the chick *unc5b* homologue and its expression during avian embryonic development. Sequence homology between chick and mouse *unc5b* was high, and expression patterns in developing chick and mouse embryos appeared highly conserved as well. In particular, we found little *unc5b* expression in the nervous system of young chick or quail embryos, as previously seen in the mouse (Engelkamp, 2002; Lu et al., 2004). Chick *unc5b* was prominently expressed on arterial EC and sprouting vessels during the period of active angiogenesis in developing avian embryos. Quiescent vessels of the CAM at late embryonic stages down regulated *unc5b*, but re-expression was induced by activation of vessel sprouting following grafts of tumor cells on the CAM. This vascular expression pattern is highly similar to the one described in the mouse, where *unc5b* is expressed in arterial EC and sprouting vessels during embryonic development, becomes down regulated during postnatal life but is re-expressed during pathological neovessel sprouting, as seen in oxygen-induced retinopathy and tumor angiogenesis (Larrivee et al., 2007; Lu et al., 2004). Taken together, these data show that UNC5B is an evolutionary conserved vascular receptor.

Previous work has shown that UNC5B is a repulsive receptor for the axon guidance molecule Netrin-1 (Hong et al., 1999; Larrivee et al., 2007; Leonardo et al., 1997; Lu et al., 2004). To investigate repulsive or attractive actions of Netrin-1 during vascular development, we have used protein or cell-based delivery of Netrin-1 to avian embryos at various stages of development. We found that delivery of Netrin-1 protein to the CAM led to plasma leakage, followed by formation of fibrous nodules and reorganization of the CAM vasculature. Similar observations have previously been reported (Park et al., 2004) and were interpreted to reflect 'attractive' or pro-angiogenic responses of Netrin-1 on CAM blood vessels. However, we found that the primary response to Netrin-1 is rapid plasma leakage from vessels, suggesting that all subsequent events, i.e., fibrous nodule formation and vessel reorganization are likely to be secondary consequences of the plasma leak, perhaps induced by liberation of inflammatory mediators. The mechanism by which Netrin-1 induced plasma leak requires further investigation. As Netrin-1 induces retraction of EC expressing UNC5B *in vitro* (Larrivee et al., 2007), one possibility is that Netrin-1 could induce similar retraction of CAM vessels expressing low levels of UNC5B, thereby generating inter-endothelial gaps allowing plasma leak. However, alternative possibilities cannot be excluded and require further investigation.

In contrast to acute protein delivery, slower release of Netrin-1 by HEK or human tumor cells

grafted onto the CAM did not result in plasma leakage and allowed us to test effects on CAM vessel sprouting. Of four matched pairs of cell lines transfected or retrovirally transduced with control vectors or Netrin-1 encoding vectors, all four Netrin-1 expressing cell lines showed reduced sprouting of *unc5b* expressing vessels into the nodules formed from the grafted cells, concomitant with a reduction in overall angiogenesis and growth. Thus, Netrin-1 appears to repel UNC5B expressing chick blood vessels, suggesting that the function of UNC5B as a repulsive receptor contributing to vessel patterning during vessel morphogenesis is also conserved in evolution.

While all Netrin-1 expressing cell lines showed reduced sprouting of *unc5b* expressing vessels, the overall effect on angiogenesis and nodule growth varied between the different cell lines. The most drastic effect was observed with HEK cells secreting relatively high levels of cNetrin-1, which were virtually devoid of vessels and formed only tiny nodules on the CAM, while control HEK cells were well vascularized and HEK cells expressing mVEGF formed large, well vascularized nodules. Mel2A melanoma cells and PC3 cells secreting 10 or 50 times less hNetrin-1 compared to HEK cNetrin-1 cells also showed a significant reduction in overall angiogenesis and growth. In PC3 tumors, the anti-angiogenic effect of hNetrin-1 was delayed compared to Mel2A tumors, perhaps related to the lower hNetrin-1 secretion requiring longer time for sufficient protein accumulation in the matrix. However, MiaPaCa pancreatic tumor cells, which secreted similar amounts of hNetrin-1 compared to Mel2A cells, showed only a transient reduction in angiogenesis and no growth reduction compared to control-transduced cells. The reason for this behavior is currently unclear, but may relate to cell-specific cues that could influence Netrin-receptor interactions. Of note, the human tumor cell lines used in the chick CAM model have been previously analyzed by xenografting into nude mice (Larrivee et al., 2007). The reduction in angiogenesis and growth observed in the chick model recapitulates growth and vascularization patterns seen in nude mice, i.e., significant inhibition of vascularization and growth with Mel2A and PC3 Netrin-1 expressing cells compared to control-transduced tumors, and angiogenesis inhibition, but no growth reduction with MiaPaCa cells. These results highlight the usefulness of the chick CAM model to evaluate tumor growth and angiogenesis, as it is rapid, cheap and does not require surgical interventions in adults (Hagedorn et al., 2005). In addition, the different tumor cell lines each exhibit reproducible and characteristic growth patterns and histology, reminiscent of the embryonic origin of the cell lines, with ectomesodermal Mel2A cells growing on the surface of the CAM and endomesodermal MiaPaCa and PC3 cells growing towards the endoderm, suggesting that the CAM may represent a favorable environment to recapitulate

aspects of endogenous growth of these tumors.

In addition to monitoring tumor growth and vascularization, we analyzed the participation of CEC/EPC to tumor angiogenesis in the presence or absence of Netrin-1 using the quail/chick parabiosis model. We observed that $QH1^+$ CEC/EPC colonized tumors formed from all cell lines and attained a density similar to the one found in other tissues of parabiotic embryos (Pardanaud and Eichmann, 2006). As CEC/EPC numbers never exceeded 3.3% of total intratumoral EC, their incorporation is unlikely to directly contribute to neovessel growth in this model. EPC involvement in tumor angiogenesis is debated because the contribution of EPC to tumor neovessels varies considerably depending on tumor models (Shaked et al., 2005). While some studies show important integration of EPC, others claim that these cells do not integrate into the endothelium and promote angiogenesis only indirectly (Vajkoczy et al., 2003; Larrivee et al., 2005; Urbich and Dimmeler, 2004a). CEC/EPC may serve a structural bridging role or may secrete paracrine growth factors to support tumorigenesis (Urbich and Dimmeler, 2004b; Zentilin et al., 2006). Netrin-1 expression did not significantly alter CEC/EPC incorporation, indicating that the repulsive effect of this factor on EC is restricted to vascular sprouts expressing *unc5b*.

Examination of *unc5b* expression during early embryonic development showed strong expression in mesodermal cells of the posterior primitive streak and the cardiac crescent. This expression pattern is similar to the one seen with *vegfr2*, which labels angioblasts and hemangioblasts (Eichmann et al., 1997), suggesting that at least some of the *unc5b* expressing cells could be angioblasts. However, expression patterns of *vegfr2* and *unc5b* diverge at later developmental stages: while *vegfr2* labels angioblasts as they exit from the primitive streak and migrate to form the primary vascular plexus, *unc5b* is not detectable in angioblasts of the primary vascular plexus and only becomes detectable in EC once these have formed arteries, i.e., the dorsal aorta and vitelline artery. In agreement with the absence of *unc5b* expression, grafts of Netrin-1 expressing cells during these stages failed to repel or otherwise influence migrating angioblasts. In mouse mutants deficient for *unc5b*, the equivalent stages of vascular development proceeded normally, while sprouting of arterial side branches was abnormal (Lu et al., 2004), arguing that UNC5B function is not required for vasculogenesis, but required for proper patterning and formation of angiogenic sprouts. In summary, we found that unc5b expressing vessels in avian embryos were repelled after stimulation by Netrin-1, confirming and extending our previous observations in mice (Lu et al., 2004, Larrivée et al., 2007). In contrast, we did not observe any pro-angiogenic effects of Netrin-1 in any experiment performed in this study, while these could be readily detected in all

experiments with the known pro-angiogenic factor VEGF. Thus, while an ectopic source of Netrin-1 may stimulate ischemic revascularization processes during adult neovascularization (Wilson et al., 2006), ectopic Netrin-1 does not appear to act as a pro-angiogenic factor during avian embryonic development.

Figure legends

Fig. 1. *Unc5b* expression in the avian embryo

A-D: Whole-mount ISH with an *unc5b* antisense riboprobe on quail embryos at the indicated somite stages. Ventral (A-C) and dorsal (D) views, anterior is to the left. *Unc5b* is expressed in the cardiac crescent (A, arrowhead) and in mesoderm of posterior primitive streak (A-D, arrows). Arterial *unc5b* is detected at the 21 somite stage in the forming vitelline arteries (D, arrowheads). Asterisks in C, D indicate non-specific signal inside the neural tube. E, F: Comparison between *unc5b* (E) and *vegfr2* (F) expression on E3 chick embryo transverse sections. The two genes are exclusively transcribed in EC but *unc5b* expression (E) is restricted to the arterial system including the dorsal aorta (Ao) and sprouting segmental arteries (arrows). *Unc5b* mRNA is not transcribed in the cardinal vein (CV) and only on some migrating angioblasts (arrowhead, E). *Vegfr2* is expressed everywhere in the vascular system (F) including aorta, sprouting segmental arteries (arrows) and migrating angioblasts (arrowheads, F). G-J: *Unc5b*/QH1 double staining on transverse sections of E3.5 (G) and E5.5 (H) quail embryos and E12 quail CAM (I, J). G: Co-expression of QH1 and *unc5b* in EC of a sprouting segmental artery (arrows). Note lower *unc5b* levels in the aortic endothelium and absence of labeling of an isolated angioblast (arrowhead). H: In the limb bud, arterial EC express *unc5b* (arrows) while venous EC (arrowheads) do not. I: In a quiescent CAM, *unc5b* is down regulated in arteries (A) and veins (V). J: Stimulation of CAM neovessel sprouting by grafting of a tumor (T) leads to *unc5b* up regulation on angiogenic sprouts invading the tumor (arrows) but not in the quiescent CAM vessels underneath the tumor (*). Scale bars: A-D: 0,5 mm; E, F: 35 µm; G, H: 15 µm; I, J: 10 µm.

Fig. 2: Netrin-1 induces plasma leakage of CAM vessels

A-C: Bright field pictures illustrating the chick CAM after application of the indicated factors inside silicone rings (R). A: Vascular plexus after application of control protein (PBS-0.1% BSA), note normal aspect of CAM vessels. B: Recombinant hVEGF induces neovessel sprouting. C: Fibrous nodule (arrow) formed after application of recombinant cNetrin-1. D-F: Intravascular injection with FITC-dextran. D: 15 minutes after recombinant cNetrin-1 application, plasma leakage is observed and amplified after 30 minutes (E). F: Vessel perfusion of the same CAM as in D, E, but outside the application area. Note that perfusion is normal, indicating that vessel leakage is confined to the area treated with Netrin-1. Bars: A-C: 800 µm; D-F: 200 µm.

Fig. 3: Vascularization and growth of HEK cells expressing Netrin-1 or VEGF on the CAM A-C: Bright field pictures illustrating the macroscopic aspect of the indicated HEK cells 6 days after grafting on the quail CAM. A: Control cells spread over the CAM region inside the silicone ring (R) and form a flat disc. B: Necrotic nodule formed from HEK Netrin-1 cells. C: HEK VEGF cells develop large vascularized nodules. D, E: Histograms showing counts of total numbers of $QH1^+$ EC inside the nodules (D) and nodule size (E) at 3 and 6 days after grafting. *: $p<0.05$ at 3 and 6 days after grafting compared to HEK control. F-H: QH1/glychemalun staining of nodules 3 days after grafting. F: HEK control cells are vascularized by capillaries (arrows) sprouting from CAM vessels. G: HEK Netrin-1 nodules appear mostly necrotic while the underlying CAM is dilated and filled with inflammatory cells (brown dots). Note that the CAM vessels (arrowheads) are located far from the grafted nodule. H: HEK VEGF nodules contain numerous $QH1^+$ vessels (arrows). Bars: A-C: 2.2 mm; F-H: 110 μm.

Fig. 4: Vascularization and growth of human tumor cells on chick CAM of parabioses A-C: Bright field pictures showing a ventral view of the indicated neo-transduced tumors 6 days after grafting. R = silicone ring; Arrows in B= folding up of the tumor. D-F: General histological aspect of different tumors, dorsal side is up. D: Mel2A tumors (T) grow as sheets on top of the CAM. Note that, while the CAM endoderm is present (arrowhead), the ectodermal layer is absent at the tumor surface. E: Note folding up of the endoderm and formation of diverticuli (arrows) in MiaPaCa tumors. F: PC3 tumors grow towards the endoderm and form hemorrhagic vesicles (V) that break (blue arrowhead) and liberate erythrocytes to the CAM surface (black arrow). Black arrowhead= CAM. G-I: QH1/Glychemalun staining of tumor sections to illustrate vessel morphology. G: Mel2A tumor vessels (arrows) sprout radially from CAM vessels (arrowheads). H: MiaPaCa tumor capillaries (black arrows) derived from CAM vessels (black arrowheads) have a larger lumen than Mel2A tumor vessels and are filled with erythrocytes. Blue arrow: Interstitial $QH1^+$ CEC/EPC. Blue arrowhead: $QH1^+$ HC. Asterisks: lymphatics. I: A PC3 intratumoral vesicle (V) contains avian erythrocytes (black arrowheads) and two $QH1^+$ quail HC (arrow) as well as PC3 cells (blue arrowheads) which have a larger nucleus than the avian cells. At the edges of the vesicle, chick capillaries (C) are filled with avian erythrocytes. J, K: Histograms showing counts of total numbers of EC inside the nodules (J) and nodule size (K) at 3, 6 or 7 days after grafting. The number of grafts performed for each cell line is indicated in J. *: $p<0.05$. Bars: A-C: 900 μm; D-F: 800 μm; G-I: 50 μm.

Fig. 5. CEC/EPC mobilization during tumor angiogenesis

A-C: QH1/glychemalun double staining of representative tumor sections illustrating participation of CEC/EPC to neovascularization. A: An isolated EC found in the tumor interstitium (arrowhead). B: An isolated QH1 EC integrated into a tumor neovessel (arrowhead). C: A QH1 HC in the tumor interstitium (arrowhead). D: Histograms showing number of total intratumoral $QH1^+$ CEC/EPC. Note low numbers of CEC/EPC in all 6 tumor cell lines analyzed (compare with 4J). Bar: A-C: 15 μm.

Fig. 6. Unc5b expression during tumor neovascularization

A-D: *Unc5b* (blue) QH1 (brown) double staining on sections of tumors formed by the indicated cell lines 3 days after grafting on the quail CAM. Note robust invasion of the neo-transduced tumors by $QH1^+$/*unc5b* expressing vessel sprouts (A, C, arrowheads), while $QH1^+$/*unc5b* sprouts are scarce in Netrin-1 transduced tumors (B, D, arrowheads). Bars: A, B: 160 μm; C, D: 22 μm.

Fig. 7. Netrin-1 reduces migration of somite-derived EC

A: Schematic representation of the experimental procedure. Left panel illustrates an E2 chick transverse section with Neural tube (blue) Notochord (orange) Somite (black circle) Aortae (red) Endoderm and Ectoderm (black lines). Medial panel: host axial structures are removed (blue arrow) together with one somite (black arrow), which is replaced by its quail counterpart (dotted line). Right panel: Control, Netrin-1-or VEGF-expressing cell aggregate is grafted in place of axial structures. B: Illustration of the operation, the neural tube (NT) and the notochord (NC) have been partially removed. One somite of the left has been removed (asterisk) and will be replaced by a quail somite. The cell mass will be grafted later on. S: Somite. C: Quantification of the percentage of $QH1^+$ EC migrating to the contralateral side. The number of grafts performed is indicated. D, E, F: Truncal transverse sections 2 days after the operation stained with QH1/glychemalun. The midline is illustrated by a dotted line. D: Representative picture at the level of the ablation, neural tube and notochord are absent while a grafted cell mass is in place (dashed area). $QH1^+$ EC can be seen on the grafted side (brown staining), but no quail EC have migrated to the contralateral side in this image. E: Rostrally to the ablation site, HEK control cells do not impair the migration of $QH1^+$ EC to the contralateral side (arrowhead). F: HEK- Netrin-1 producing cells reduce $QH1^+$ EC migration to the contralateral side (arrowhead). Bars: B: 205 □m; C-E: 120 □m.

Fig. 8. Netrin-1 has no effect on vasculogenesis

A-C: Whole-mount QH1 immunostaining of E2 quail embryos 12 hours after the indicated grafts. Note abundant $QH1^+$ EC surrounding a VEGF bead (A). B: A Mel2A/neo transduced cell aggregate in contact with $QH1^+$ EC (arrows). C: Mel2A/Netrin-1 expressing cell aggregates at a distance from $QH1^+$ EC (arrows). D: Transverse section of an E2 quail embryo 12 hours after grafting of a Mel2A/Netrin-1 aggregate; QH1/glychemalun staining. Human cells have a larger nucleus than quail cells. $QH1^+$ EC surround the graft (arrows). Boxed area: Low magnification illustrating the graft location in the lateral mesoderm. E: Quantification of the number of EC surrounding the grafts, number of grafts is indicated. Bars: A: 30 μm, B-C: 15 μm, D: 25 μm.

References

Chisholm, A. and Tessier-Lavigne, M. (1999). Conservation and divergence of axon guidance mechanisms. Curr. Opin. Neurobiol. 9, 603-15.
Cirulli, V. and Yebra, M. (2007). Netrins: beyond the brain. Nat. Rev. Mol. Cell. Biol. 8, 296-306.
Conway, E. M., Collen, D. and Carmeliet, P. (2001). Molecular mechanisms of blood vessel growth. Cardiovasc. Res. 49, 507-21.
Dickson, B. J. (2002). Molecular mechanisms of axon guidance. Science 298, 1959-64.
Drake, C. J., LaRue, A., Ferrara, N. and Little, C. D. (2000). VEGF regulates cell behavior during vasculogenesis. Dev. Biol. 224, 178-88.
Drake, C. J. and Little, C. D. (1995). Exogenous vascular endothelial growth factor induces malformed and hyperfused vessels during embryonic neovascularization. Proc. Natl. Acad. Sci. U S A 92, 7657-61.
Eichmann, A., Marcelle, C., Breant, C. and Le Douarin, N. M. (1996). Molecular cloning of Quek 1 and 2, two quail vascular endothelial growth factor (VEGF) receptor-like molecules. Gene 174, 3-8.
Engelkamp, D. (2002). Cloning of three mouse Unc5 genes and their expression patterns at mid-gestation. Mech. Dev. 118, 191-7.
Gerhardt, H., Golding, M., Fruttiger, M., Ruhrberg, C., Lundkvist, A., Abramsson, A., Jeltsch, M., Mitchell, C., Alitalo, K., Shima, D. et al. (2003). VEGF guides angiogenic sprouting utilizing endothelial tip cell filopodia. J. Cell. Biol. 161, 1163-77.
Hagedorn, M., Javerzat, S., Gilges, D., Meyre, A., de Lafarge, B., Eichmann, A. and Bikfalvi, A. (2005). Accessing key steps of human tumor progression in vivo by using an avian embryo model. Proc. Natl. Acad. Sci. U S A 102, 1643-8.
Hong, K., Hinck, L., Nishiyama, M., Poo, M. M., Tessier-Lavigne, M. and Stein, E. (1999). A ligand-gated association between cytoplasmic domains of UNC5 and DCC family receptors converts netrin-induced growth cone attraction to repulsion. Cell 97, 927-41.
Isogai, S., Horiguchi, M. and Weinstein, B. M. (2001). The vascular anatomy of the developing zebrafish: an atlas of embryonic and early larval development. Dev. Biol. 230, 278-301.
Kennedy, T. E. (2000). Cellular mechanisms of netrin function: long-range and short-range actions. Biochem. Cell. Biol. 78, 569-75.
Klessinger, S. and Christ, B. (1996). Axial structures control laterality in the distribution pattern of endothelial cells. Anat. Embryol. (Berl) 193, 319-30.
Larrivee, B., Freitas, C., Trombe, M., Lv, X., Delafarge, B., Yuan, L., Bouvree, K., Breant, C., Del Toro, R., Brechot, N. et al. (2007). Activation of the UNC5B receptor by Netrin-1 inhibits sprouting angiogenesis. Genes Dev. 21, 2433-47.
Larrivee, B., Niessen, K., Pollet, I., Corbel, S. Y., Long, M., Rossi, F. M., Olive, P. L. and Karsan, A. (2005). Minimal contribution of marrow-derived endothelial precursors to tumor vasculature. J. Immunol. 175, 2890-9.
Leonardo, E. D., Hinck, L., Masu, M., Keino-Masu, K., Ackerman, S. L. and Tessier-Lavigne, M. (1997). Vertebrate homologues of C. elegans UNC-5 are candidate netrin receptors. Nature 386, 833-8.
Lu, X., Le Noble, F., Yuan, L., Jiang, Q., De Lafarge, B., Sugiyama, D., Breant, C., Claes, F., De Smet, F., Thomas, J. L. et al. (2004). The netrin receptor UNC5B mediates guidance events controlling morphogenesis of the vascular system. Nature 432, 179-86.
Moyon, D., Pardanaud, L., Yuan, L., Breant, C. and Eichmann, A. (2001). Plasticity of endothelial cells during arterial-venous differentiation in the avian embryo. Development 128, 3359-70.

Noden, D. M. (1988). Interactions and fates of avian craniofacial mesenchyme. Development 103 Suppl, 121-40.
Nolan, D. J., Ciarrocchi, A., Mellick, A. S., Jaggi, J. S., Bambino, K., Gupta, S., Heikamp, E., McDevitt, M. R., Scheinberg, D. A., Benezra, R. et al. (2007). Bone marrow-derived endothelial progenitor cells are a major determinant of nascent tumor neovascularization. Genes Dev. 21, 1546-58.
Pardanaud, L., Altmann, C., Kitos, P., Dieterlen-Lievre, F. and Buck, C. A. (1987). Vasculogenesis in the early quail blastodisc as studied with a monoclonal antibody recognizing endothelial cells. Development 100, 339-49.
Pardanaud, L. and Eichmann, A. (2006). Identification, emergence and mobilization of circulating endothelial cells or progenitors in the embryo. Development 133, 2527-37.
Pardanaud, L., Luton, D., Prigent, M., Bourcheix, L. M., Catala, M. and Dieterlen-Lievre, F. (1996). Two distinct endothelial lineages in ontogeny, one of them related to hemopoiesis. Development 122, 1363-71.
Park, K. W., Crouse, D., Lee, M., Karnik, S. K., Sorensen, L. K., Murphy, K. J., Kuo, C. J. and Li, D. Y. (2004). The axonal attractant Netrin-1 is an angiogenic factor. Proc. Natl. Acad. Sci. U S A 101, 16210-5.
Shaked, Y., Bertolini, F., Man, S., Rogers, M. S., Cervi, D., Foutz, T., Rawn, K., Voskas, D., Dumont, D. J., Ben-David, Y. et al. (2005). Genetic heterogeneity of the vasculogenic phenotype parallels angiogenesis; Implications for cellular surrogate marker analysis of antiangiogenesis. Cancer Cell 7, 101-11.
Shirasaki, R., Mirzayan, C., Tessier-Lavigne, M. and Murakami, F. (1996). Guidance of circumferentially growing axons by netrin-dependent and -independent floor plate chemotropism in the vertebrate brain. Neuron 17, 1079-88.
Urbich, C. and Dimmeler, S. (2004a). Endothelial progenitor cells: characterization and role in vascular biology. Circ. Res. 95, 343-53.
Urbich, C. and Dimmeler, S. (2004b). Endothelial progenitor cells functional characterization. Trends Cardiovasc. Med. 14, 318-22.
Vajkoczy, P., Blum, S., Lamparter, M., Mailhammer, R., Erber, R., Engelhardt, B., Vestweber, D. and Hatzopoulos, A. K. (2003). Multistep nature of microvascular recruitment of ex vivo-expanded embryonic endothelial progenitor cells during tumor angiogenesis. J. Exp. Med. 197, 1755-65.
Wilson, B. D., Ii, M., Park, K. W., Suli, A., Sorensen, L. K., Larrieu-Lahargue, F., Urness, L. D., Suh, W., Asai, J., Kock, G. A. et al. (2006). Netrins promote developmental and therapeutic angiogenesis. Science 313, 640-4.
Wilting, J., Christ, B., Bokeloh, M. and Weich, H. A. (1993). In vivo effects of vascular endothelial growth factor on the chicken chorioallantoic membrane. Cell Tissue Res. 274, 163-72.
Wong, T. S. and Ordahl, C. P. (1996). Troponin T gene switching is developmentally regulated by plasma-borne factors in parabiotic chicks. Dev. Biol. 180, 732-44.
Zentilin, L., Tafuro, S., Zacchigna, S., Arsic, N., Pattarini, L., Sinigaglia, M. and Giacca, M. (2006). Bone marrow mononuclear cells are recruited to the sites of VEGF-induced neovascularization but are not incorporated into the newly formed vessels. Blood 107, 3546-54.

Fig. 1

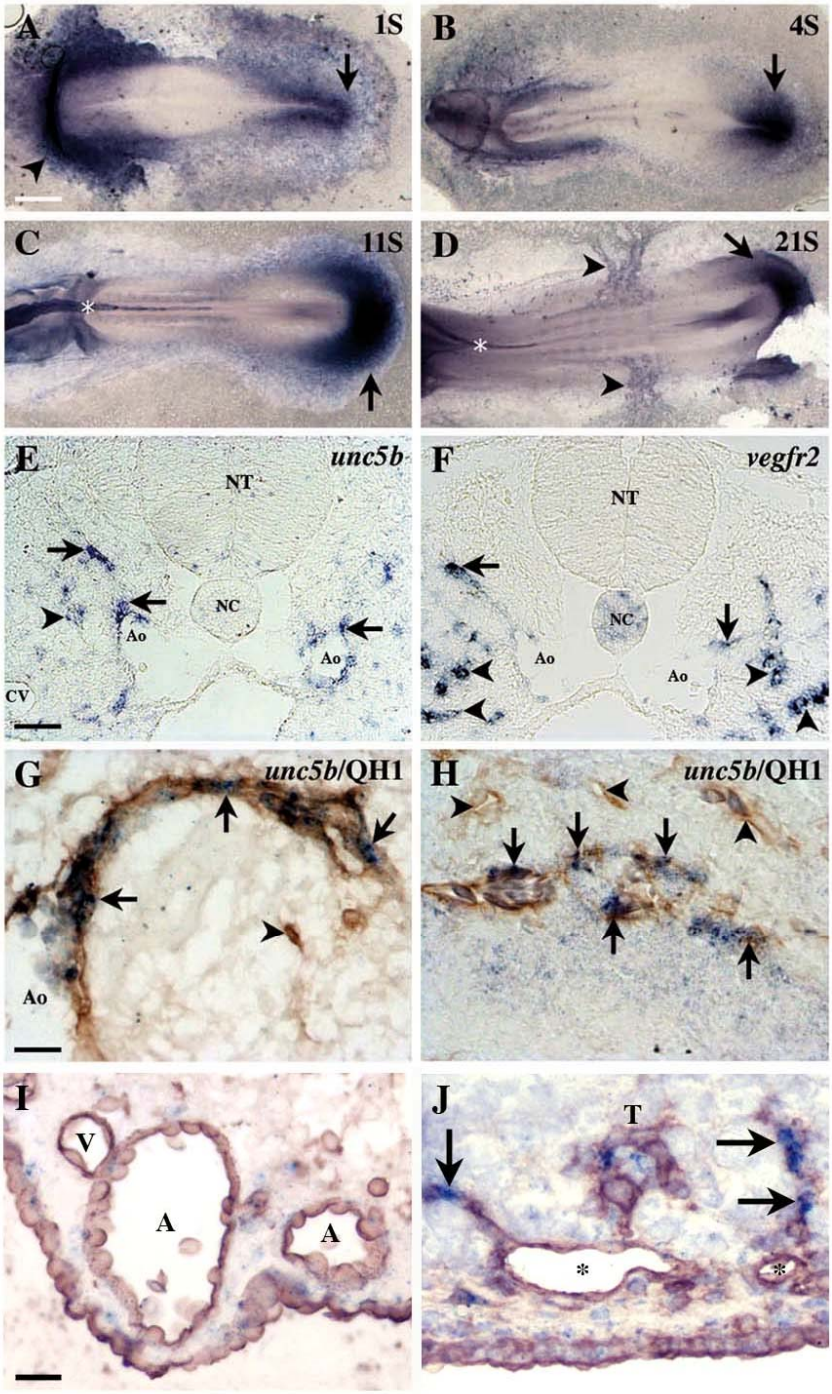

Fig. 2

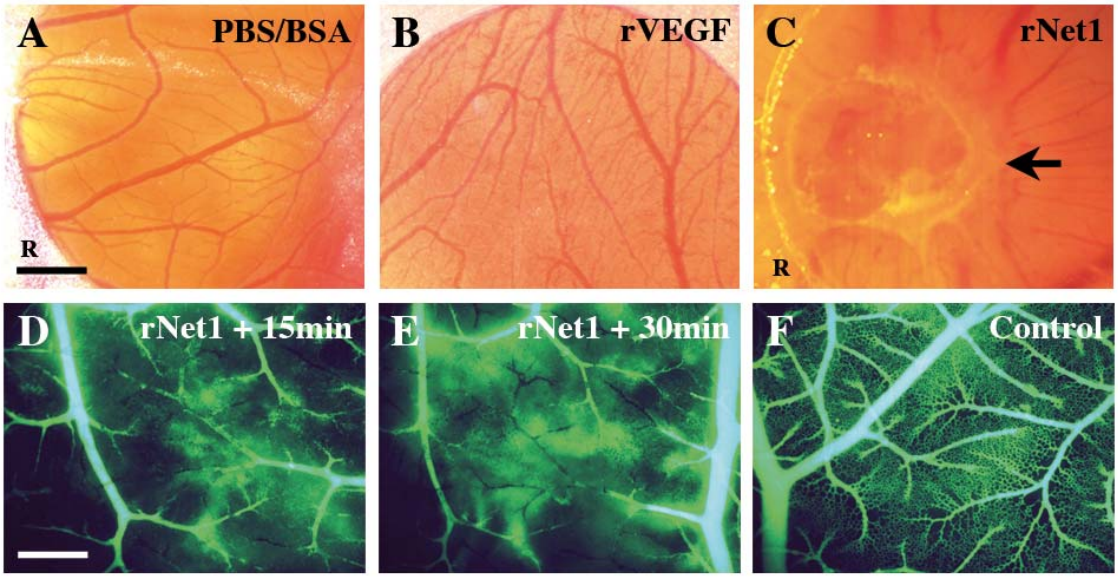

Fig. 3

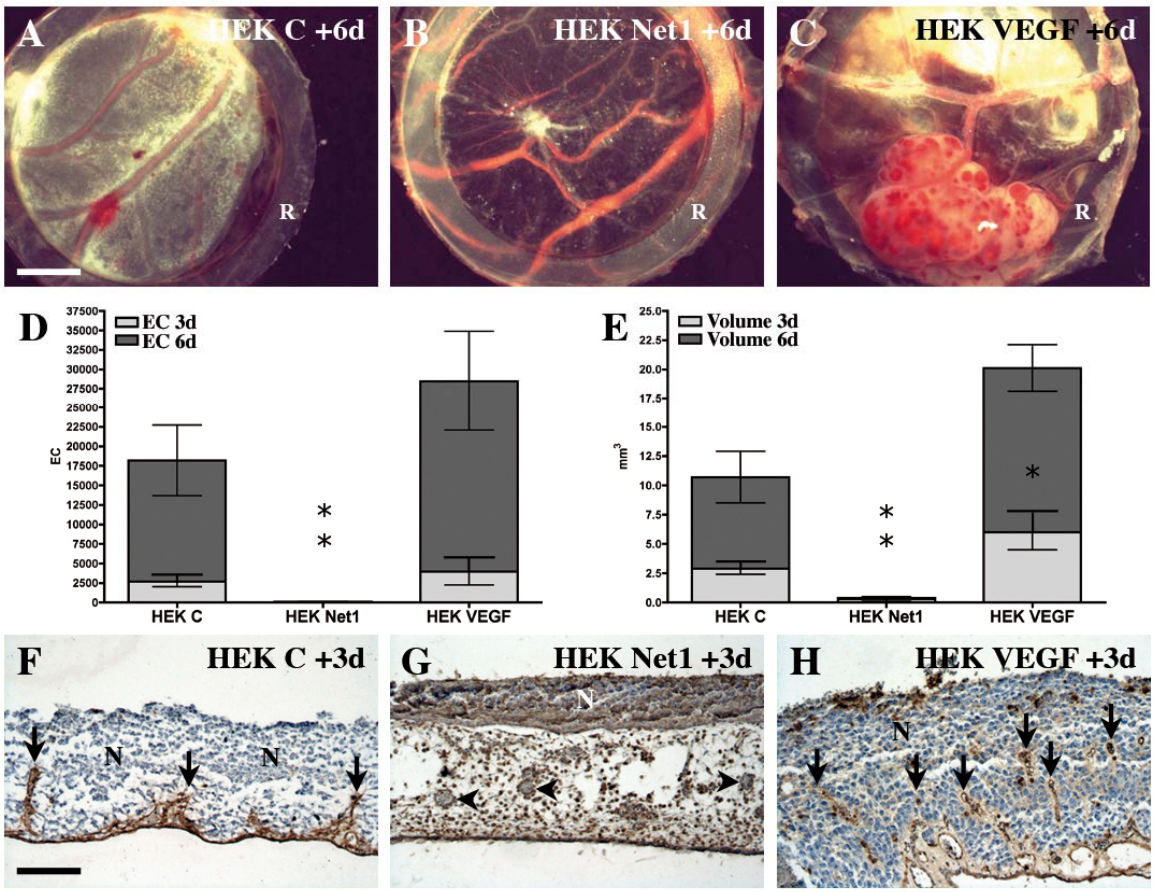

Fig. 4

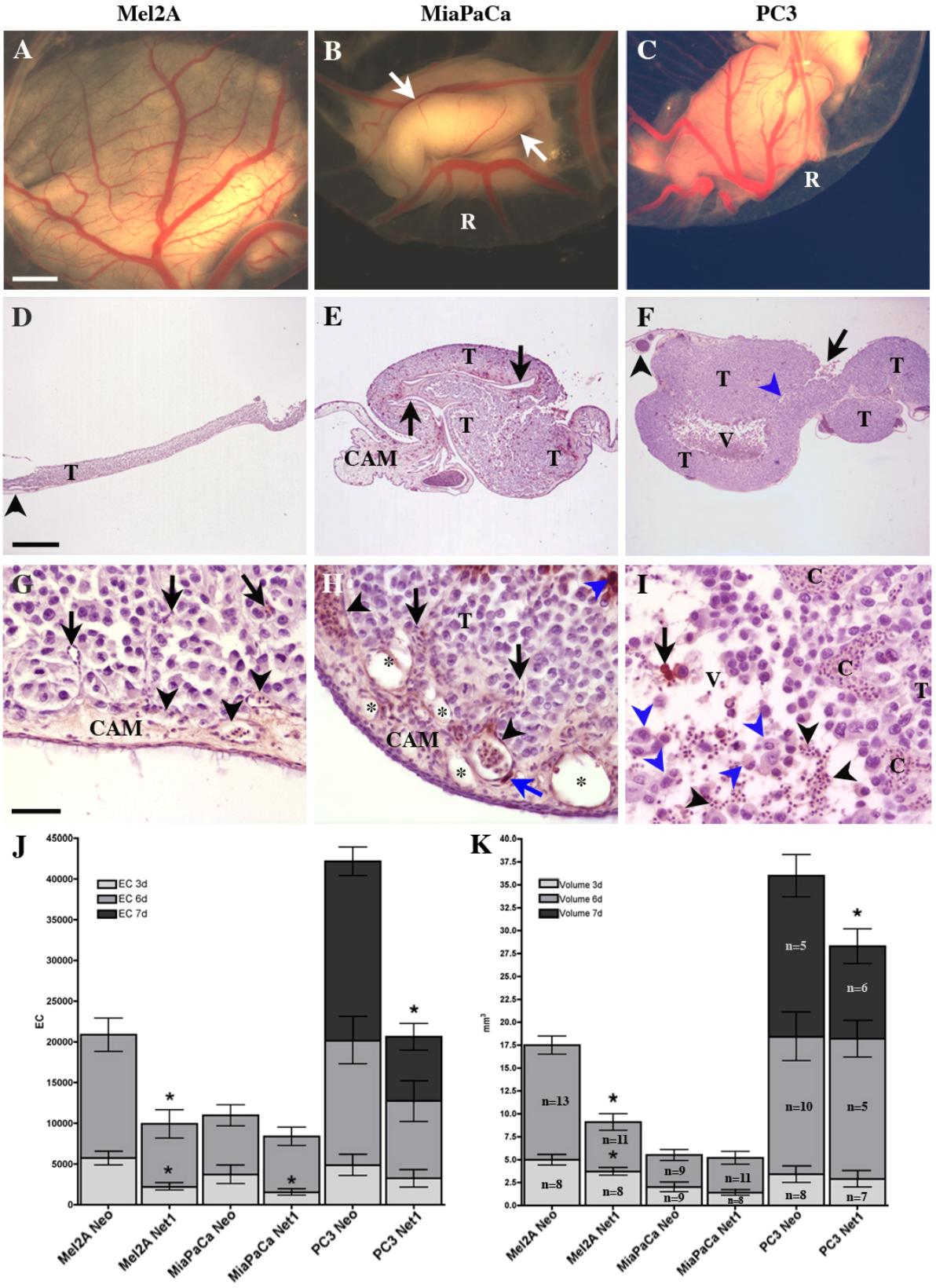

Fig. 5

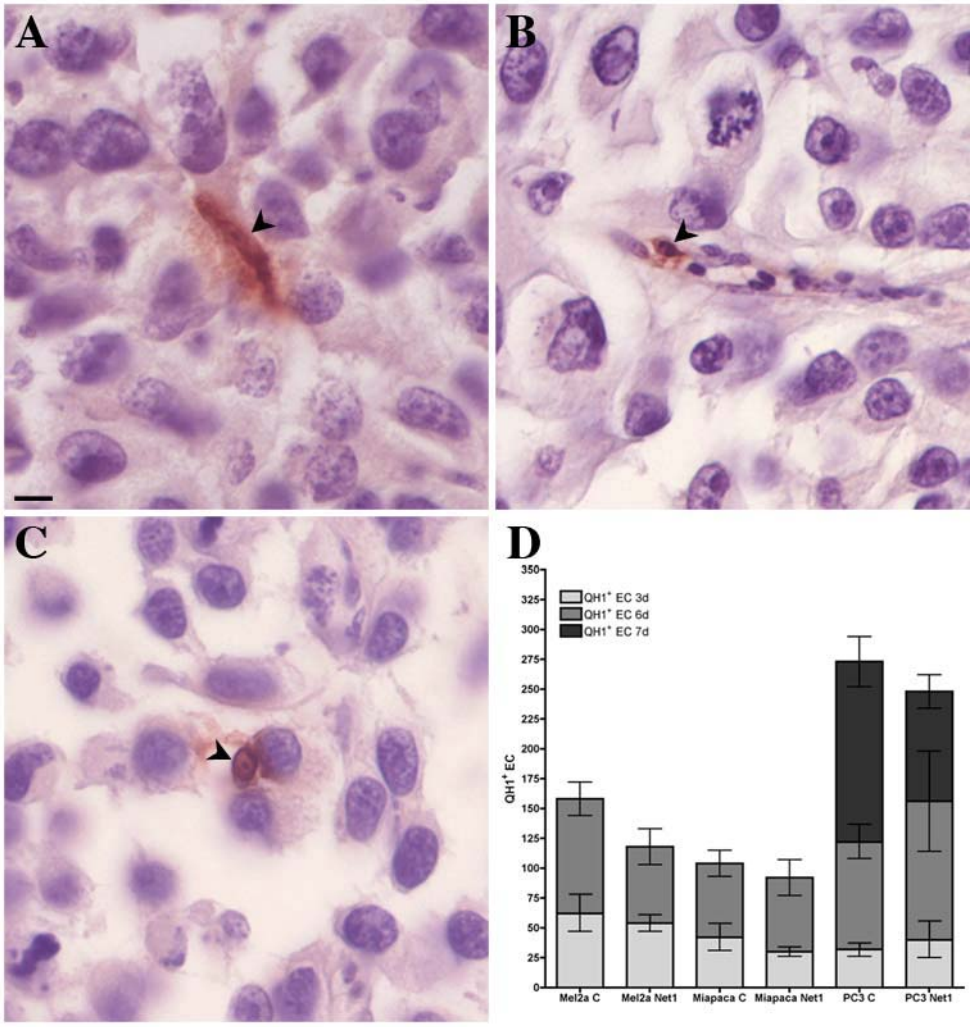

Fig. 6

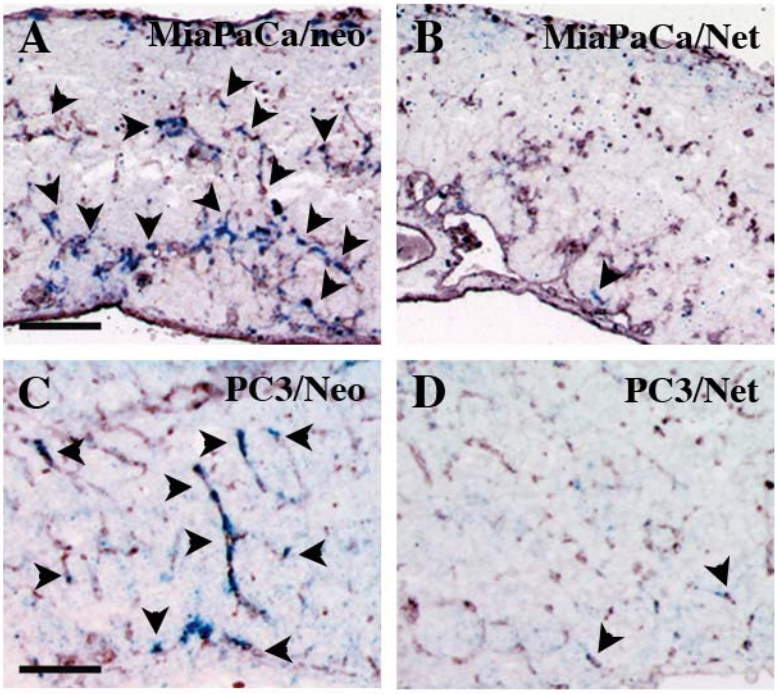

Fig. 7

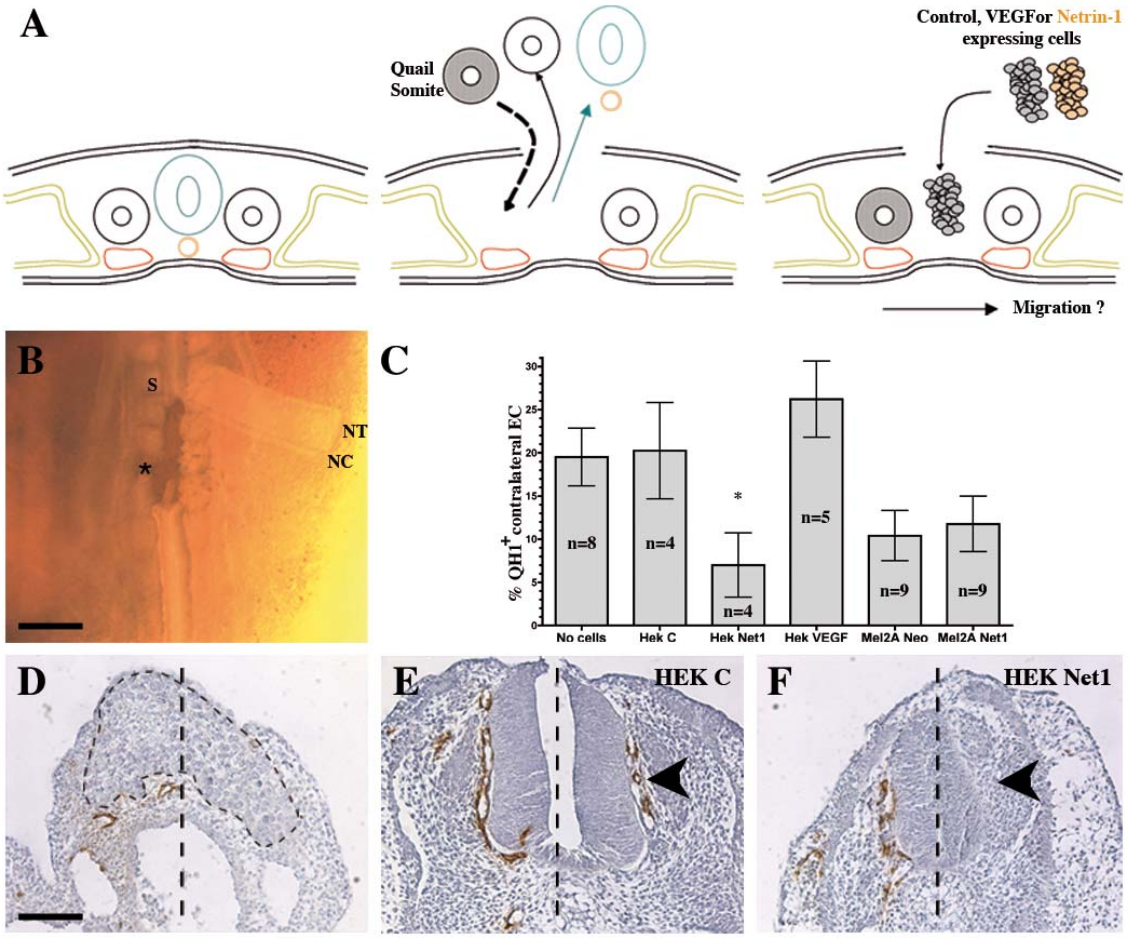

Fig. 8